

Electronic Supplementary Information for

**Revealing anisotropic strain in exfoliated graphene by polarized Raman spectroscopy**

Cheng-Wen Huang,<sup>a</sup> Ren-Jye Shiue,<sup>b</sup> Hsiang-Chen Chui,<sup>ac</sup> Wei-Hua Wang,<sup>b</sup> Juen-Kai Wang,<sup>bd</sup> Yonhua Tzeng,<sup>ce</sup> Chih-Yi Liu\*<sup>acf</sup>

<sup>a</sup> *Department of Photonics, National Cheng Kung University, Tainan 70101, Taiwan. Fax: +886-6-2095040; Tel: +886-6-2363243; E-mail: chihiliu@mail.ncku.edu.tw*

<sup>b</sup> *Institute of Atomic and Molecular Sciences, Academia Sinica, P.O. Box 23-166, Taipei 10617, Taiwan*

<sup>c</sup> *Advanced Optoelectronic Technology Center, National Cheng Kung University, Tainan 70101, Taiwan*

<sup>d</sup> *Center for Condensed Matter Sciences, National Taiwan University, Taipei 10617, Taiwan*

<sup>e</sup> *Institute of Microelectronics, National Cheng Kung University, Tainan 70101, Taiwan*

<sup>f</sup> *Department of Electrical Engineering, National Cheng Kung University, Tainan 70101, Taiwan*

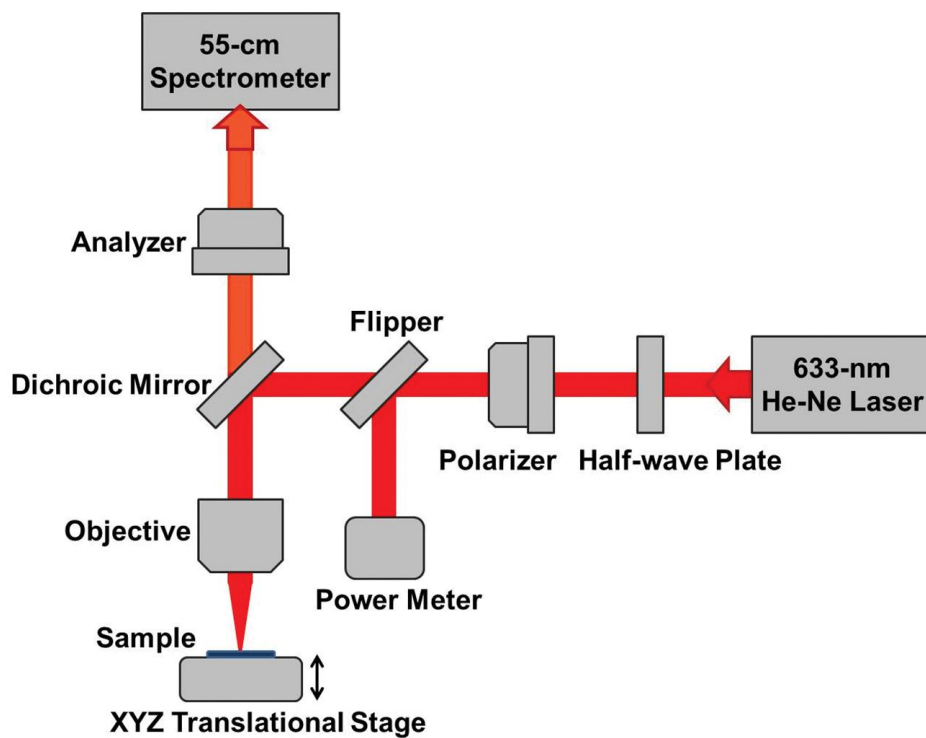


**Fig. S1** Schematic diagram showing the optical system for Raman measurements.

## Analysing Fig. 2 by a uniaxial strain model

In the literature, several groups have explored strain in graphene by artificially bending the sample.<sup>1,2</sup> This process creates a uniaxial tensile strain parallel to the bending direction and another weaker compressive strain perpendicular to that based on the Poisson effect. The polarized Raman spectrum of the graphene G mode contains two red-shifted sub-peaks compared to the unstrained one. The spectrum change with polarization is somewhat similar to what is shown in Fig. 2. Therefore, we intuitively proposed a uniaxial strain model to approach the polarization dependence seen in Fig. 2. In this model, we speculated a uniaxial strain splitting the G peak into two shifted sub-peaks in addition to the unstrained ( $G_0$ ) peak, with the resulting spectrum being the combination of all three. The two sub-peaks are named as  $G_+$  and  $G_-$  based on their differences in position. To simplify the study, the spectra with the maximum and minimum peak positions in Fig. 2 were analysed first, exemplified by what is displayed in Fig. S2. Fig. S2a shows the G peaks under  $\Phi$  of  $270^\circ$  and  $360^\circ$ , where  $\Phi$  is the included angle between the incident and scattered direction of polarization. We assumed the peak for the minimum ( $\Phi$  of  $360^\circ$ ) to be a mixture of  $G_0$  and  $G_-$ , while that for the maximum ( $\Phi$  of  $270^\circ$ ) is a combination of  $G_0$  and  $G_+$ . Subtracting the spectrum for a  $\Phi$  of  $270^\circ$  from that for a  $\Phi$  of  $360^\circ$  leads to a mixture of  $G_-$  and reversed  $G_+$  peaks, as shown in Fig. S2b. Using a double-Lorentzian function to fit the subtracted spectrum leads to a  $G_-$  peak of  $1573\text{ cm}^{-1}$  and a  $G_+$  of  $1586\text{ cm}^{-1}$ . According to the literature,<sup>2</sup> the frequencies of the two modes can be expressed as

$$\omega_+ = \omega_0 - \omega_0\gamma(1-\nu)\varepsilon + \frac{1}{2}\beta\omega_0(1+\nu)\varepsilon \quad (\text{S1})$$

$$\omega_- = \omega_0 - \omega_0\gamma(1-\nu)\varepsilon - \frac{1}{2}\beta\omega_0(1+\nu)\varepsilon \quad (\text{S2})$$

where  $\omega_0$ ,  $\nu$ , and  $\varepsilon$  are the unstrained G mode frequency, Poisson ratio (= 0.13), and uniaxial strain, respectively.  $\gamma$  (= 1.99) is the Grüneisen parameter, while  $\beta$  (= 0.99) is the shear deformation potential. Inserting the  $G_-$  position ( $\omega_-$ ) of  $1573\text{ cm}^{-1}$  and  $G_+$  position ( $\omega_+$ ) of  $1586\text{ cm}^{-1}$  in equations S1 and S2, we found  $\omega_0 = 1600\text{ cm}^{-1}$  and  $\varepsilon = 0.73\%$ . The  $\omega_0$  of  $1600\text{ cm}^{-1}$  is far from the known G peak position of  $1580\text{ cm}^{-1}$ ,<sup>3</sup> and is thus unreasonable. In addition, it is doubtful that the graphene is under a strain as

large as 0.73%, which is usually caused by an artificial action, such as bending the sample. Therefore, the uniaxial strain model is inappropriate to explain our experimental results. Note that the authors in reference 2 used a Poisson ratio different from ours. Their experiment is based on bending a flexible substrate with a graphene film fixed on the surface. The deformation of the graphene is dominated by the substrate and thus they used the Poisson ratio of the substrate in their calculation. The adhesion between the graphene and substrate is weaker in our experiment and thus using the Poisson ratio of graphene but not the substrate is adequate.

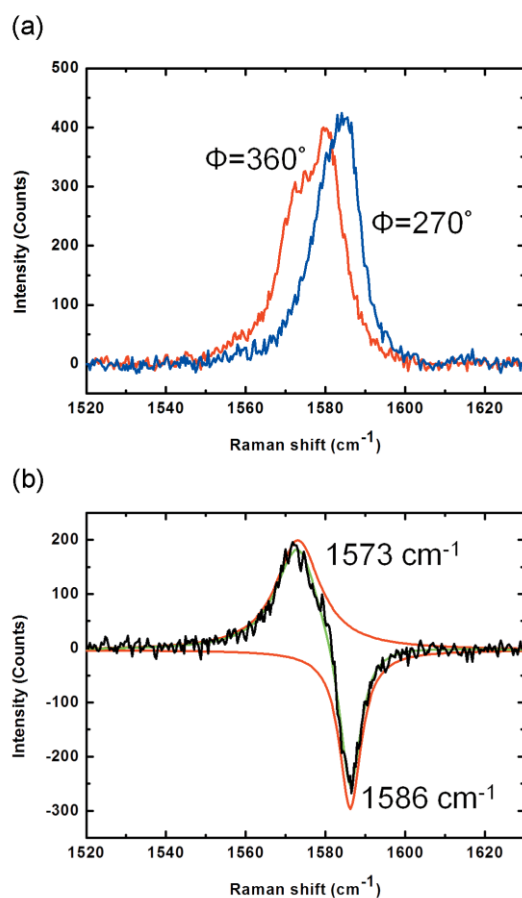


**Fig. S2** (a) Polarized Raman spectra of graphene under  $\Phi$  of  $270^\circ$  (blue curve) and  $360^\circ$  (red curve). (b) The plot (black curve) that results after subtracting the spectrum for a  $\Phi$  of  $270^\circ$  from that for a  $\Phi$  of  $360^\circ$ . After the subtraction, the remainder (black curve) was fitted by a double-Lorentzian function, whose two peaks are shown by the red curves. The green curve displays the sum of the two red ones.

**Table S1** Detailed information on the parameters (averages) used in the triple-Lorentzian function fitting for Fig. 4.

Polarization angle (deg)	$G_{-}$		$G_0$		$G_{+}$	
	Peak position (cm <sup>-1</sup> )	Full width at half maximum (cm <sup>-1</sup> )	Peak position (cm <sup>-1</sup> )	Full width at half maximum (cm <sup>-1</sup> )	Peak position (cm <sup>-1</sup> )	Full width at half maximum (cm <sup>-1</sup> )
0	1572.5	11.5	1580.2	7.4	None	None
90	None	None	1580.0	12.8	1585.5	7.2
180	1572.9	11.8	1580.5	7.5	None	None
270	None	None	1580.6	11.2	1585.9	6.1
360	1572.7	11.6	1580.7	8.1	None	None
<b>Average</b>	1572.7	11.6	1580.4	9.4	1585.7	6.7

To determine the parameters, we exploited double-Lorentzian functions to fit the spectra whose G peaks hold the maximum or minimum peak positions in Fig. 2. In this way, we obtained several sets of peak positions and full widths at half maxima (FWHMs) for the  $G_{-}$ ,  $G_0$ , and  $G_{+}$  modes. Their positions and FWHMs were averaged as the parameters for triple-Lorentzian fitting.

## Detailed derivation of Equation 1

This derivation refers to a more general case reported by M. Hugan *et al.*<sup>1</sup> Here, the optical measurement geometry is schematically depicted in Fig. 5. The vector describing the atomic displacement in the strained G band is given by:

$$\vec{v} = \begin{bmatrix} \cos \Phi_s \\ \sin \Phi_s \end{bmatrix} \quad (\text{S3})$$

The Raman tensors of the unstrained G mode are written as:

$$R_x = \begin{bmatrix} 0 & 1 \\ 1 & 0 \end{bmatrix} \quad (\text{S4})$$

$$R_y = \begin{bmatrix} 1 & 0 \\ 0 & -1 \end{bmatrix} \quad (\text{S5})$$

Therefore the Raman tensors for the strained G mode are described by:

$$R = v_x R_x + v_y R_y = \begin{bmatrix} \sin \Phi_s & \cos \Phi_s \\ \cos \Phi_s & -\sin \Phi_s \end{bmatrix} \quad (\text{S6})$$

The incident and scattered polarization vectors,  $\mathbf{e}_i$  and  $\mathbf{e}_s$ , are expressed as:

$$\vec{e}_i = \begin{bmatrix} \cos(\Theta_i + \Phi_s) \\ \sin(\Theta_i + \Phi_s) \end{bmatrix} \quad (\text{S7})$$

$$\vec{e}_s = \begin{bmatrix} \cos(\Theta_s + \Phi_s) \\ \sin(\Theta_s + \Phi_s) \end{bmatrix} \quad (\text{S8})$$

We employ the polarization dependence for the Raman scattering relation of  $I = A|\mathbf{e}_i \mathbf{R} \mathbf{e}_s|^2$ , where A is a constant. Then the Raman intensity (I) of the strained G mode is written as

$$I = A \sin^2(\Theta_i + \Theta_s + 3\Phi_s) \quad (\text{S9})$$

Equation S9 is identical to Equation 1.

### A local strain analysis based on double-Lorentzian fitting

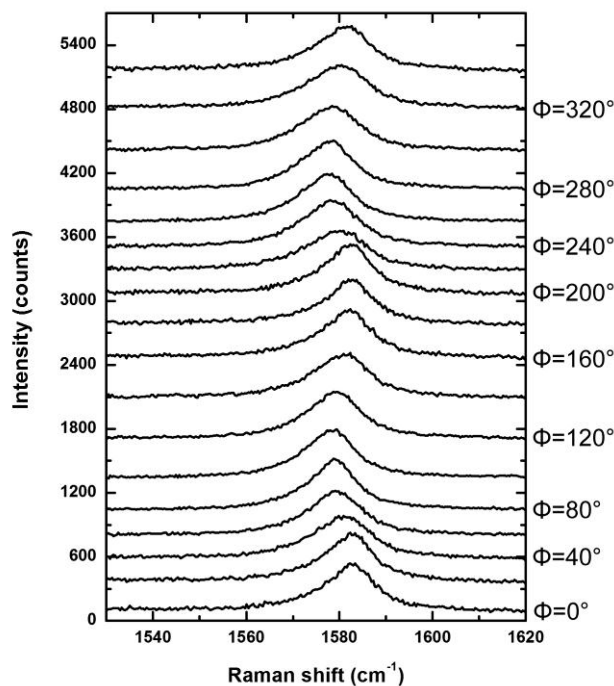


**Fig. S3** Polarized Raman spectra of G modes varying with the polarization angle of the excitation light ( $\Phi$ ). The  $\Phi$ 's with an interval of  $20^\circ$  are the inclined angles between the incident and scattered polarization directions.

Figure S3 shows polarized Raman spectra, whose optical geometrical optical geometry is similar to what is shown in Fig. 5, from a graphene sample different from that for Fig. 2. Similar to Fig. 2, the spectral profile of the G mode evolves noticeably as the  $\Phi$  changes. However, the peaks for the maximum and minimum positions are symmetric and thus are fitted by single- but not double-Lorentzian functions, such as Fig. S4a displays. Fitting all the extreme spectra indicates the average peak centre is  $1582.0 \text{ cm}^{-1}$  (named as  $G_+$ ) for the maxima and  $1577.8 \text{ cm}^{-1}$  (named as  $G_-$ ) for the minima. Every spectrum in Fig. S3 can be properly fitted by two Lorentzian functions with centres of  $G_+$  and  $G_-$ , as exemplified by Fig. S4b. Therefore it is reasonable that the G peak for any  $\Phi$  is composed of  $G_+$  and  $G_-$  sub-modes. Figure S5a and b show that the dependencies of the integrated intensities of both  $G_+$  and  $G_-$  peaks— $I(G_+)$  and  $I(G_-)$ , respectively—on  $\Phi$  undergo periodic variations with a relative shift of  $\sim 90^\circ$ , while  $I(G_+) + I(G_-)$  remains fairly constant (Fig. S5c). In other words, the integrated intensity of the G

peak is independent of the measurement geometry, but those of the corresponding two sub-peaks are geometry-dependent. In addition, the variations in  $I(G_+)$  and  $I(G_-)$  are  $\sim 90^\circ$  out of phase, which implies the two peaks are correlated with different directional characters.

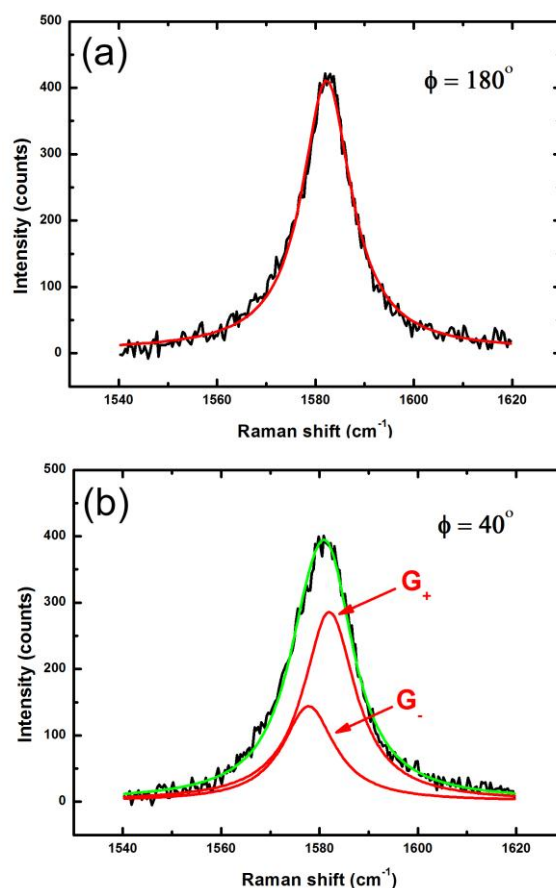


**Fig. S4** (a) Fitting the G peak with a Lorentzian function for  $\Phi$  of  $180^\circ$ , which corresponding to one of the maximum peak positions in Fig. S3. (b) Fitting the G peak for  $\Phi$  of  $180^\circ$  with a double-Lorentzian function whose two peaks correspond to  $1582.0 \text{ cm}^{-1}$  ( $G_+$ ) and  $1577.8 \text{ cm}^{-1}$  ( $G_-$ ). The red curves represent the fitted peaks of the corresponding spectra. The black curves display the spectra while the green one shows a profile by adding all the related fitting peaks.

According to a discussion similar to that for Fig. 4, the  $G_+$  is caused by a compression, while the  $G_-$  is caused by a tension. Equation 2 properly fits the intensity variations in Fig. S5a and b, as shown by the corresponding black curves. To be noted, the parameter ‘A’ for equations 2 is selected as the average of  $I(G_+) + I(G_-)$  for different  $\Phi$  because the integrated intensity of the G peak is independent of the



measurement geometry (Fig. S5c). Equation 3 is used to determine the strain for  $G_+$  of -0.06% and  $G_-$  of 0.07%. The analysis presented here implies local strain in a graphene film can be variable in different areas or samples and choosing a proper Lorentzian function form is needed for fitting.

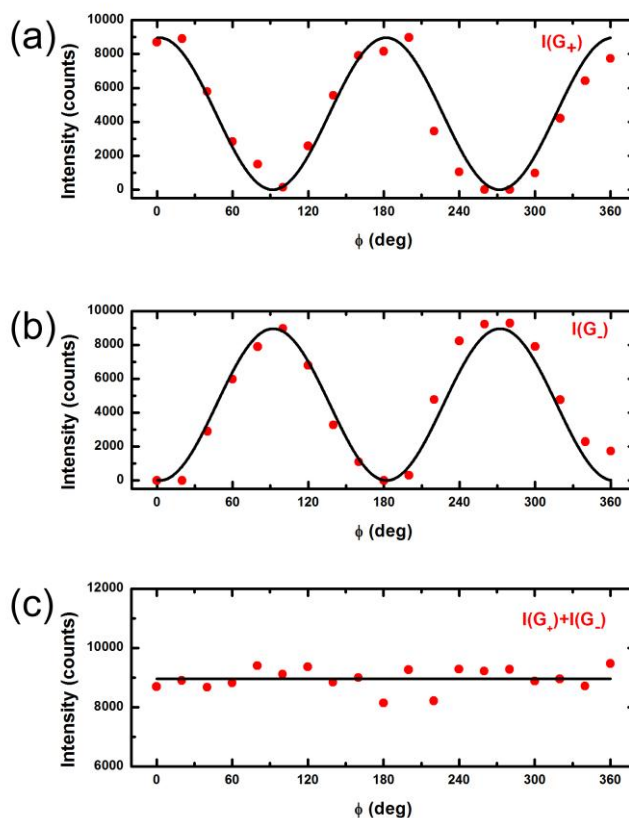


**Fig. S5** The plots of (a)  $I(G_+)$ , (b)  $I(G_-)$ , and (c)  $I(G_+) + I(G_-)$  as functions of  $\Phi$ . The symbol “I” denotes the intensity of the corresponding sub-peak, obtained by fitting the related Raman spectrum with a double-Lorentzian function. The obtained intensities are shown by the red dots, which are fitted using  $A \sin^2(\Phi - \Phi_s)$  for (a) and (b) and a constant of A for (c), where A and  $\Phi_s$  are fitting parameters. The black lines display the fitting results.

## References

- 1 M. Y. Huang, H. G. Yan, C. Y. Chen, D. H. Song, T. F. Heinz and J. Hone, *Proc. Natl. Acad. Sci. U. S. A.*, 2009, **106**, 7304-7308.
- 2 T. M. G. Mohiuddin, A. Lombardo, R. R. Nair, A. Bonetti, G. Savini, R. Jalil, N. Bonini, D. M. Basko, C. Galiotis, N. Marzari, K. S. Novoselov, A. K. Geim and A. C. Ferrari, *Phys. Rev. B*, 2009, **79**, 205433.
- 3 Y. Y. Wang, Z. H. Ni, T. Yu, Z. X. Shen, H. M. Wang, Y. H. Wu, W. Chen and A. T. S. Wee, *J. Phys. Chem. C*, 2008, **112**, 10637-10640.